Letter

Field-driven spatiotemporal manipulation of Majorana zero modes in a Kitaev spin liquid

Chihiro Harada⬤, Atsushi Ono⬤, and Joji Nasu⬤
Department of Physics, Tohoku University, Sendai 980-8578, Japan

The Kitaev quantum spin liquid possesses two fractional quasiparticles, itinerant Majorana fermions and localized visons. It provides a promising platform for realizing a Majorana zero mode trapped by a vison excitation. This local mode behaves as a non-Abelian anyon capable of applications to quantum computation. However, creating, observing, and manipulating visons remain challenging even in the pristine Kitaev model. Here, we propose a theory to control visons enabled by a time-dependent local magnetic field in the Kitaev spin liquid. Examining the time evolution of the magnetic state, we demonstrate that a vison follows a locally applied field sweeping in the system. We clarify that one can move a vison accompanied by a Majorana zero mode by choosing the velocity and shape of the local field appropriately. In particular, the controllability of visons using local fields shows nonlinear behavior for its strength, which originates from interactions between Majorana fermions and visons. The present results suggest that itinerant Majorana fermions other than zero modes play a crucial role in vison transport. Our finding will offer a guideline for controlling Majorana zero modes in the Kitaev quantum spin liquid.

Electron correlations in solids bring about exotic ground states with strong quantum entanglement, and resultant elementary excitations possess completely different natures from electrons. Amongst others, elementary excitations behaving like independent particles emergent from an electron divided are called fractional quasiparticles. Elucidating their properties is one of the main subjects in modern condensed matter physics. A representative example of fractional quasiparticles is a Majorana fermion, which is identical to its own antiparticle [1]. The fractionalization into multiple Majorana quasiparticles can cause non-Abelian anyonic statistics between them, which is applied to topological quantum computation [2–5]. Therefore, manifestations of Majorana quasiparticles have been intensively investigated in many-body quantum states, such as unconventional superconductors [6–10] and fractional quantum Hall systems [11–14].

A quantum spin model proposed by Kitaev offers another platform of Majorana fermions [15]. This model, composed of simple interactions between $S = 1/2$ quantum spins, exhibits a quantum spin liquid (QSL) as its ground state. Elementary excitations from the QSL are described by two fractional quasiparticles: Majorana fermions and local excitations termed visons [16–22]. Under magnetic fields, the Majorana fermion system is topologically nontrivial, which results in a Majorana fermion with zero energy, called a Majorana zero mode, bound by each vison. This composite quasiparticle behaves as a non-Abelian anyon similar to a zero-energy Majorana state trapped by a vortex in superconductors. Recent extensive investigations have clarified that the Kitaev model can be realized in transition metal compounds [23–28], metal-organic frameworks [29], and cold atom systems [30–33]. In particular, the half-integer quantized thermal Hall effect inherent to topological Majorana fermions has been reported to be observed in the ruthenium compound α-RuCl$_3$ under magnetic fields [34–37]. While the presence

of the quantization has still been under debate [38–40], this material is believed to be a promising candidate for the Kitaev QSL with non-Abelian anyons. For applications of the Kitaev systems to quantum computing, one needs to create, observe and manipulate vison excitations as desired. Several proposals for observing visons have been made via scanning tunneling microscope (STM) and atomic force microscope measurements [41–48] and interferometry for Majorana edge modes [49–51] in this context. However, less is known about how to manipulate a vison with a Majorana zero mode, even in the pristine Kitaev model.

In this Letter, we theoretically propose a way to control visons using a local magnetic field in the Kitaev QSL. We introduce the Kitaev model under a weak uniform magnetic field. This field makes each vison excitation accompanied by a Majorana fermion but does not invest itinerant nature to visons. Here we show that visons can be spatiotemporally manipulated by applying a local field sweeping across the system. We also reveal optimal conditions of the moving velocity and intensity of the local field to control a vison. Furthermore, we find a nonlinearity for the local field caused by interactions between itinerant Majorana fermions and visons, which are crucial for vison manipulations.

We start from the Kitaev model under a uniform magnetic field as follows [15]:

$$\mathcal{H}_K = -J \sum_{\langle jj' \rangle_\gamma} S_j^\gamma S_{j'}^\gamma - \kappa \sum_{\langle\langle jj'j'' \rangle\rangle_{\gamma\gamma'\gamma''}} S_j^\gamma S_{j'}^{\gamma'} S_{j''}^{\gamma''}, \quad (1)$$

where S_j^γ is the γ component of an $S = 1/2$ spin at site j on a honeycomb lattice. The first term represents the bond-dependent Ising-type interaction between spins on nearest neighbor (NN) γ bond $\langle jj' \rangle_\gamma$ ($\gamma = x, y, z$) [Fig. 1(a)] with the exchange constant J, and the second term stands for an effective field leading to a chiral spin liquid with a
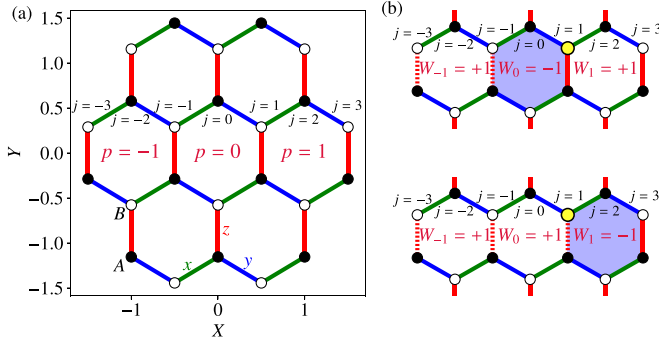
FIG. 1. (a) Honeycomb lattice cluster with open boundaries including $N = 24$ spins on which the Kitaev model is defined. Blue, green, and red lines represent the x, y, and z bonds, respectively, and filled (open) circles stand for sites belonging to the A (B) sublattice. The origin of the spatial coordinate is taken at the center of the cluster, and each hexagon is labeled by p with the central hexagon as $p = 0$ and numbered along the X direction. In a similar manner, sites are numbered with j along xy bonds toward the X direction such that the uppermost site of the central hexagon with $p = 0$ is $j = 0$. (b) Two flux configurations with a vison at $p = 0$ and 1 associated with Z_2 variables with $\eta_r = -1$ on the z bonds shown by dashed lines. The matrix element of S^z on the yellow site ($j = 1$) is nonzero between two flux configurations.

topologically nontrivial gap. The latter is given as the product of three spins on neighboring three sites $\langle\langle jj'j''\rangle\rangle_{\gamma\gamma'\gamma''}$ consisting of γ and γ'' bonds with γ' being neither γ nor γ''. This term has been proposed to originate from higher-order perturbations for the Zeeman term [15] and Γ' interactions [52,53] and has been discussed as an independent term from magnetic fields [54–57]. By performing the Jordan-Wigner transformation along chains composed of x and y bonds, we can rewrite Eq. (1) using two Majorana fermions c_j and $\bar{c}_j$ at each site as [58–63]

$$\mathcal{H}_K = -\frac{J}{4}\sum_{[jj']_x} ic_jc_{j'} - \frac{J}{4}\sum_{[jj']_y} ic_jc_{j'} - \frac{J}{4}\sum_{[jj']_z} \eta_r ic_jc_{j'}$$
$$- \frac{\kappa}{8}\sum_{\langle\langle jj'j''\rangle\rangle_{zxy}} \eta_r ic_jc_{j''} - \frac{\kappa}{8}\sum_{\langle\langle jj'j''\rangle\rangle_{xyz}} \eta_r ic_jc_{j''}$$
$$- \frac{\kappa}{8}\sum_{\langle\langle jj'j''\rangle\rangle_{yzx}} ic_jc_{j''}, \qquad (2)$$

where the spin operator on sublattice A (B) is given by $(S_j^x, S_j^y, S_j^z) = \frac{1}{2}(c_j\tau_j, -\bar{c}_j\tau_j, ic_j\bar{c}_j) [\frac{1}{2}(\bar{c}_j\tau_j, -c_j\tau_j, i\bar{c}_jc_j)]$ with $\tau_j = \prod_{j'<j}(-2S_{j'}^z)$ [see Fig. 1(a)]. Here, $[jj']_\gamma$ is the ordered NN pair and $\eta_r = i\bar{c}_j\bar{c}_{j'}$ on z bond r, where j (j') belongs to sublattice A (B). The quantity η_r exists also on the z bond of neighboring three sites $\langle\langle jj'j''\rangle\rangle_{zxy}$ and $\langle\langle jj'j''\rangle\rangle_{xyz}$. Since η_r commutes with $\mathcal{H}_K$ and satisfies $\eta_r^2 = 1$, it is a local Z_2 conserved quantity. We also introduce a physical local conserved quantity as $W_p = 2^6 \prod_{j\in p} S_j^{\gamma_j}$ on each hexagon plaquette p with γ_j being the bond type not belonging to the hexagon loop at site j. This quantity relates to η_r as $W_p = \eta_{r_1}\eta_{r_2}$, where r_1 and r_2 are the two z bonds on the hexagon p. The ground state of $\mathcal{H}_K$ belongs to the sector with all W_p being $+1$, called flux-free. Then, the elementary

excitations are described by two quasiparticles: itinerant Majorana fermions c_j and local excitations flipping W_p to -1. The latter quasiparticles are termed visons.

Figure 1(b) shows two single-vison excitations, where a vison is located at the endpoint of the string crossing z bonds with $\eta_r = -1$. To manipulate visons, we need to consider an external field with nonzero matrix elements between the two configurations. One of the simplest ways is introducing a local magnetic field for S_1^z at the yellow site $j = 1$ shown in Fig. 1(b) [55,64]. Since S_1^z anticommutes with η_{r_0} being the z bond connected with the site $j = 1$, it causes the hopping of a vison between neighboring hexagon plaquettes. We introduce the time-dependent local field $\mathcal{H}_h(t) = -\sum_j h_j(t)S_j^z$ for spatial and temporal control of visons.

In the present study, we apply the Hartree-Fock approximation to the Majorana fermion representation of $\mathcal{H} = \mathcal{H}_K + \mathcal{H}_h(t)$; the third, fourth, and fifth terms in Eq. (2) are decoupled as $i\bar{c}_i\bar{c}_jic_ic_j \simeq \langle i\bar{c}_i\bar{c}_j\rangle ic_ic_j + i\bar{c}_i\bar{c}_j\langle ic_ic_j\rangle - \langle i\bar{c}_i\bar{c}_j\rangle\langle ic_ic_j\rangle - ic_i\bar{c}_j\langle ic_j\bar{c}_i\rangle + \langle ic_i\bar{c}_j\rangle ic_j\bar{c}_i + ic_i\bar{c}_j\langle ic_j\bar{c}_i\rangle$ with a constant. The obtained mean-field Hamiltonian $\mathcal{H}_{MF}(t)$ is given by a following bilinear form of Majorana fermions $\{\gamma_l\} = \{c_1, c_2, \cdots, c_N, \bar{c}_1, \bar{c}_2, \cdots, \bar{c}_N\}$: $\mathcal{H}_{MF} = \frac{i}{4}\sum_{ll'} \gamma_l \mathcal{A}_{ll'}\gamma_{l'} + C$, where N is the number of sites, C is a constant, and $\mathcal{A}$ is a $2N \times 2N$ real skew symmetric matrix [65].

We calculate the time evolution based on the von Neumann equation and solve it by the fourth-order Runge-Kutta method with the step size Δt [66–69]. As an initial state at $t_{in} = 0$, we impose no local magnetic field with $\mathcal{H}_h(t_{in}) = 0$, where W_p and η_r are conserved quantities. Numerical calculations are performed with $\Delta t/J^{-1} = 0.01$ ($\hbar = 1$ is assumed) on the hexagon-type cluster with $N = 1734$, which is straightforwardly obtained by extending the cluster shown in Fig. 1(a) [65]. The width of the cluster for the X direction is 33, where the length of the primitive translation vectors is unity. We compute the expectation value of W_p and local density of states (LDOS) $g_j(\varepsilon; t)$ for the Majorana fermions c_j at site j, which is defined to satisfy the normalization $\int_0^\infty g_j(\varepsilon; t) d\varepsilon = 1$. The details are given in the Supplemental Material [65].

Here, we show the results for the time evolution of a vison in the presence of spatially and temporally dependent local field $\mathcal{H}_h(t)$. In the initial state, a vison is located at $(X, Y) = (p_{in}, 0)$ with $p_{in} = -6$, namely $W_{p_{in}} = -1$ and other W_p are $+1$ [see Fig. 2(a)]. The local field is applied for the sites $j = 2p_{in} + 1, 2p_{in} - 1, \cdots, 5$, where $j_{min} = 2p_{in} + 1$ is the upper right site of the hexagon p_{in}, as a shifted rectangular field $h_j(t) = A\mathcal{R}(t; (T + \Delta T)(j - j_{min})/2, T)$ with the amplitude A and delay time ΔT [see Fig. 2(k)]. $\mathcal{R}(t; t_0, T) = \theta(t - t_0)\theta(t_0 + T - t)$ is a rectangular function starting from t_0 with the width T and $\theta(t)$ is the Heaviside step function. We set the parameters as $A/J = 0.1$, $T/J^{-1} = 69$, $\Delta T/J^{-1} = 10$, and $\kappa/J = 0.05$. Figures 2(a)–2(e) show the snapshots of the spatial map for $\langle W_p \rangle$. We find that the vison moves to the right side by following the motion of the local field and its shape is largely intact by time evolution. Figure 2(l) shows the time evolution of the vison density D_p on the hexagons whose centers are located on the $Y = 0$ line, where $D_p = (1 - \langle W_p \rangle)/2$.
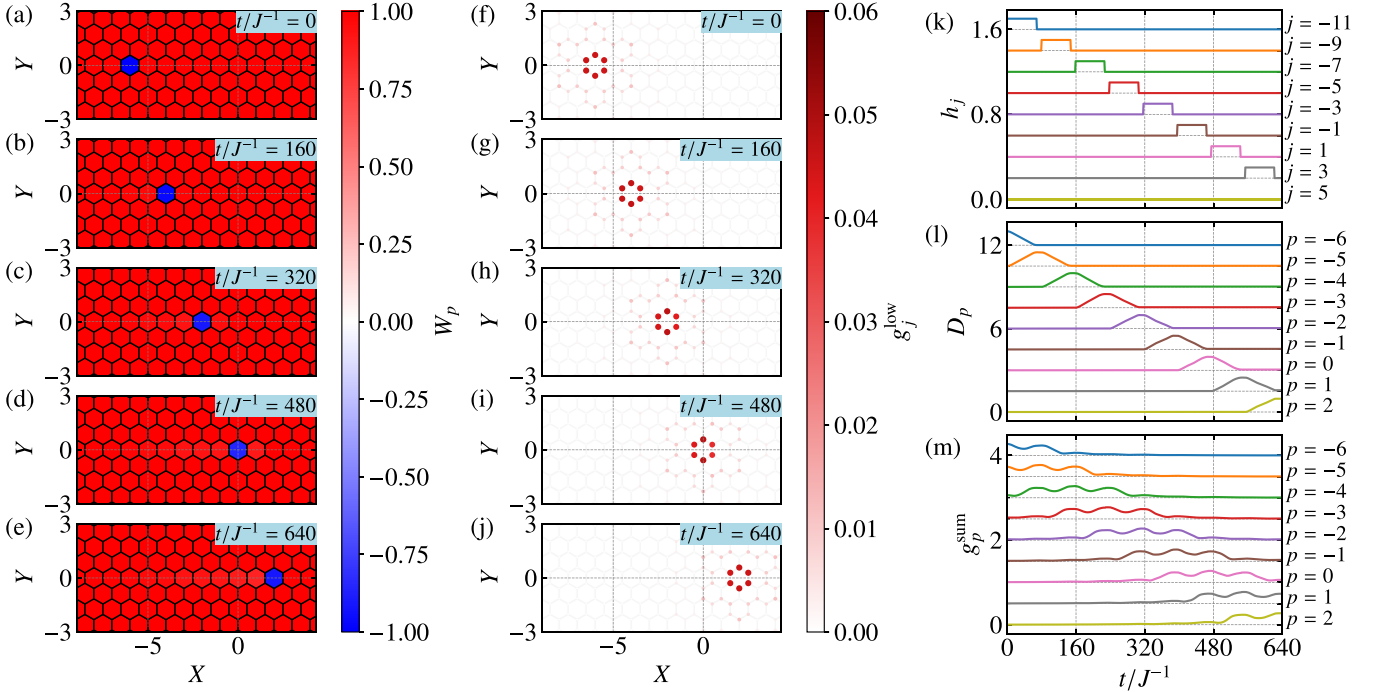
FIG. 2. (a)–(e) Spatial map of W_p under the time-dependent local field at (a) $t = 0$, (b) $t/J^{-1} = 160$, (c) $t/J^{-1} = 320$, (d) $t/J^{-1} = 480$, (e) $t/J^{-1} = 640$. (f)–(j) Corresponding figures for low-energy LDOS g_j^{low}. (j)–(m) Time evolutions of (j) the local fields h_j, (k) vison density D_p, and (m) low-energy LDOS g_p^{sum} on the hexagon plaquette p.

The NN hopping of a vison occurs while the rectangular local field is applied, and the vison almost perfectly moves to the neighboring site.

Figures 2(f)–2(j) show the snapshots of the low-energy LDOS $g_j^{low}(t)$, where $g_j^{low}(t) = \int_0^{\varepsilon_m} g_j(\varepsilon; t) d\varepsilon$ with $\varepsilon_m/J = 10^{-3}$. At $t = 0$, the large spectral weight of the low-energy LDOS is observed at the corners of the hexagon with a vison, corresponding to a Majorana zero mode. The zero mode clearly follows the vison moving to the right side while maintaining its spatial shape in time evolution. This feature is also seen in Fig. 2(m), showing the low-energy LDOS on the hexagon plaquette p, $g_p^{sum}(t) = \sum_{j \in p} g_j^{low}(t)$. The present results suggest that a vison is accompanied by a Majorana zero mode even while a time-dependent local field drives a vison. Note that this field-driven vison manipulation is sensitive to the parameters of the local field. When one changes the value of A, the wave packet of a vison spreads out and the quasiparticle picture collapses regardless of its propagation [65]. The results imply that the shape of the local magnetic field is crucial in manipulating a vison.

To examine this feature in more detail, we introduce a simple setup, where a vison is located at $p = 0$ in the initial state and the local magnetic field is applied to the spin at site $j = 1$ as a quenched field with $h_1(t) = A\theta(-t)$ [see Fig. 1(b)]. Since W_0 and W_1 do not commute with S_1^z, their expectation values should change by the local field quench. On the other hand, in the present initial condition, the relation $\langle W_0 + W_1 \rangle = 0$, namely $D_0 + D_1 = 1$, is maintained even in the presence of the local field. Figures 3(a)–3(c) show the time evolutions of D_0 and D_1 for $\kappa/J = 0.05$ for several A. In the case of $A/J = 0.06$, D_1 takes a maximum $D_1^{max} \simeq 0.2$ at $t/J^{-1} \simeq 50$

and turns to decrease and oscillate over time. On the other hand, at $A/J = 0.08$, the time evolution of D_1 exhibits a completely different behavior; the maximum value D_1^{max} reaches almost one for $A/J = 0.08$, suggesting that the hopping of a vison from $p = 0$ to $p = 1$ occurs. Further increasing A, the time evolution of D_0 and D_1 appear to be cosine-type. Note that D_1 takes a maximum at $t = t_{max} \sim 69J^{-1}$ at $A/J = 0.1$, corresponding to the time width T of the local field for controlling a vison, used in Fig. 2.
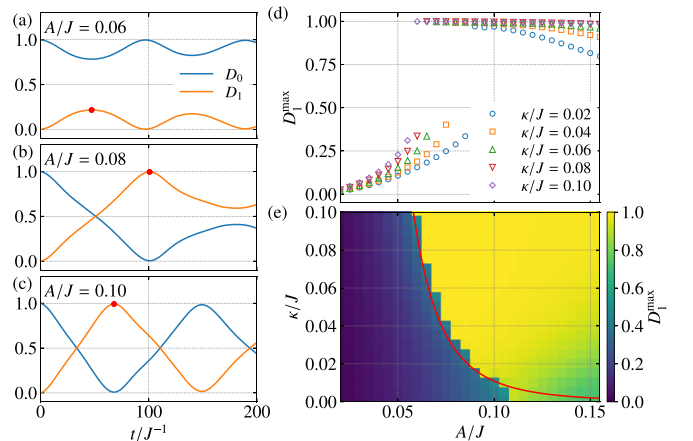

FIG. 3. (a)–(c) Time evolution of the vison densities D_p at $p = 0, 1$ after abruptly introducing the local field with (a) $A/J = 0.06$, (b) 0.08, and (c) 0.1 at the site $j = 1$ [see Fig. 1(b)]. The filled circles denote the maximum of D_1. (d) A dependence of the maximum D_1^{max} for several κ. (e) Contour plot of D_1^{max} on the A-κ plane. The red line represents $A_{cr} = 0.032\kappa^{-0.25}$.
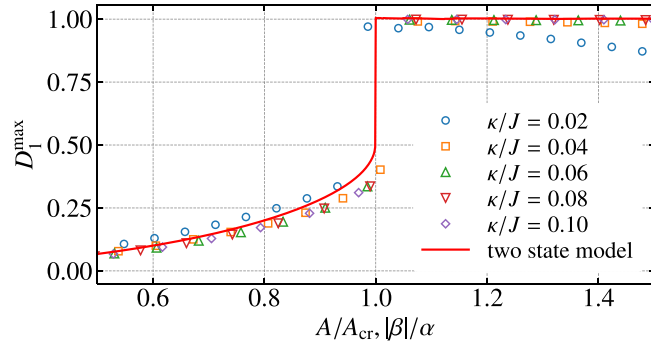
FIG. 4. Plot of $D^{\max}$ scaled by A_{cr} for the horizontal axis in Fig. 3(d). $D^{\max}$ in the two-state model is also shown by a red line as a function of $|\beta|/\alpha$.

We also find the existence of a threshold A_{cr} for the local field intensity; the vison hopping assisted by the local field does not occur below A_{cr} but the field is capable of manipulating visons above A_{cr}. The value of A_{cr} can be determined by observing the maximum of D_1, defined as $D_1^{\max}$. Figures 3(d) and 3(e) display $D_1^{\max}$ as a function of A for several κ and its contour map on the A-κ plane [70]. These results clearly show the presence of A_{cr} at which $D_1^{\max}$ abruptly changes to one. Furthermore, A_{cr} decreases with increasing κ. This result suggests that, if the background uniform field κ is weak, a stronger local field A is needed for the vison manipulation, but a weak local field can move the vison when the uniform field is strong. This is a trade-off relation between the uniform field and local field intensities. Moreover, we find $A_{cr} \simeq 0.032\kappa^{-0.25}$ by fitting A_{cr}, which is shown in Fig. 3(e) as a red line. Using the values of A_{cr}, we rescale the A dependence of $D_1^{\max}$ as presented in Fig. 4. All data almost collapse to a single curve, suggesting the presence of universal behavior in vison hoppings.

Here, we discuss the origin of the threshold behavior for the vison hopping triggered by the local field. We construct a simplified low-energy model to consider the two states presented in Fig. 1(b), where the upper and lower states are denoted as $|\Psi_0\rangle$ and $|\Psi_1\rangle$, respectively. The time-dependent wave function is written as $|\Psi(t)\rangle = c_0(t)|\Psi_0\rangle + c_1(t)|\Psi_1\rangle$ with the coefficients $c_0(t)$ and $c_1(t)$, whose time evolutions are determined by the Schrödinger equation $i\partial|\Psi(t)\rangle/\partial t = \mathcal{H}_{low}|\Psi(t)\rangle$. We assume the effective Hamiltonian $\mathcal{H}_{low}$ as the following form:

$$\mathcal{H}_{low} = \begin{pmatrix} -2\alpha\Delta(t) & \beta \\ \beta^* & 2\alpha\Delta(t) \end{pmatrix}, \qquad (3)$$

where $\Delta(t) = |c_0(t)|^2 - |c_1(t)|^2$, which causes a nonlinearity in the system. The off-diagonal terms with the coefficient β arise from the local magnetic field applied at site $j = 1$, and $|\beta|$ is expected to be given by $A|\langle\Psi_1|S_1^z|\Psi_0\rangle|$ with the local-field intensity A. On the other hand, the diagonal term with the real coefficient α mainly originates from interactions between Majorana fermions and visons intrinsic in the Kitaev model, which causes vison localization [71]. We impose $c_0(t = 0) = 1$ and $c_1(t = 0) = 0$ as initial conditions and calculate their time evolutions [65]. Since $|c_p(t)|^2$ ($p = 0, 1$) is regarded as the probability of the vison existing at p, we
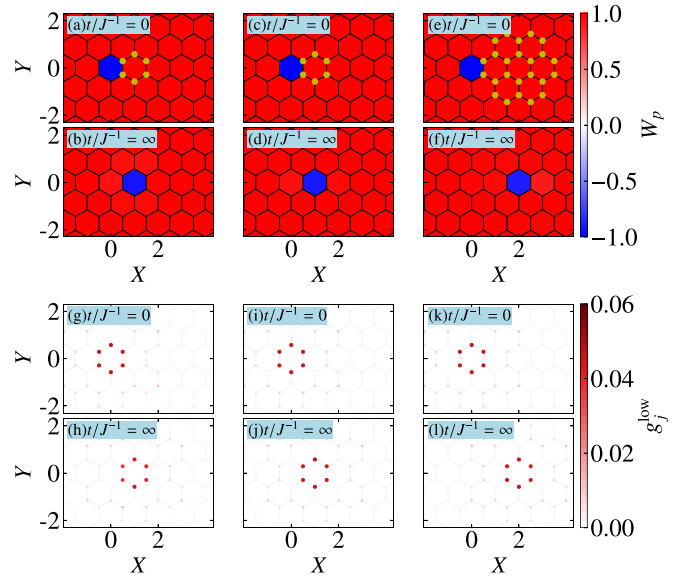

FIG. 5. (a),(b) Spatial maps of W_p (a) before and (b) after introducing the time-dependent magnetic field $h_j(t)$ applied for the six yellow sites shown in (a) as a rectangular function $A\mathcal{R}(t; 0, T)$ with $A/J = 0.04$ and $T/J^{-1} = 171$. (c)–(f) Same plots for $h_j(t)$ applied to (c),(d) the six and (e),(f) the 24 yellow sites as a Gaussian function $Ae^{-(t-t_c)^2/2\sigma^2}$ with $A/J = 0.08$, $\sigma/J = 100$ and $t_c/J^{-1} = 300$. (g)–(l) Corresponding plots to (a)–(f) for low-energy LDOS g_j^{low}. In these simulations, we set $\kappa/J = 0.05$.

assume $D_p = |c_p(t)|^2$, and $D_1^{\max}$ is determined similarly to the Hartree-Fock calculations. This quantity is plotted as a function of $|\beta|/\alpha$ in Fig. 4(b) as a red line, which exhibits a jump at $|\beta|/\alpha = 1$. The line well coincides with the Hartree-Fock results scaled by A_{cr}, implying that the low-energy two-state model can well account for the vison hopping in the lattice system.

In the case with $|\beta|/\alpha \gg 1$, the diagonal term giving the nonlinearity can be neglected and $|c_1(t)|^2 = \sin^2|\beta|t$, indicating $t_{\max} = \pi/(2|\beta|)$. The previous studies suggested $|\beta|/A = |\langle\Psi_1|S_1^z|\Psi_0\rangle| \simeq 0.23$ at $\kappa/J = 0.05$ [55,64], leading to $t_{\max}/J^{-1} \simeq 68$ for $A/J = 0.1$. The estimation of $t_{\max}$ is consistent with the Hartree-Fock result shown in Figs. 2 and 3(c). Thus far, we assume that the local magnetic field is constant for t. Even if one considers the time-dependent local field $h_1(t)$, which gives rise to the t dependence for β, the condition for $|c_1(t_{\max})|^2 = 1$ is determined only by the integral as $\int_{t_{in}}^{t_{max}} |\beta(t)|dt = \pi/2$. The result will offer a simple guideline for manipulating a vison.

To advance the practical application of vison manipulation, we investigate several variations of local fields. As illustrated in Fig. 5, a localized vison can be moved by the local fields applied to neighboring six sites as rectangular and Gaussian functions and also by the field applied even to adjacent 24 sites. These calculations suggest that visons are not additionally excited by the local fields with spatial distributions. This is interpreted as follows. When applying a local magnetic field to a specific site adjacent to a vison, the vison moves to the neighboring plaquette because the local magnetic field hybridizes two different states whose energies are degenerate. In contrast, a local field applied at a site without visons possibly

creates a pair of two visons in addition to an existing one, which demands a nonzero excitation energy [15]. Therefore, even if local magnetic fields with spatial distributions are employed beyond the field at a specific site, the excitation gap prevents the creation of visons and ensures the manipulation of a vison while preserving its shape. Furthermore, we have verified that a Majorana zero mode is always accompanied by the vison motions, as depicted in Figs. 5(g)–5(l). These results imply that the Majorana zero mode can be manipulated even by using local magnetic fields applied to multiple sites in wider regions beyond the application only to a specific site.

Within our framework, the required local-field strength and the upper limit of its sweeping speed are estimated at ~ 1 T and ~ 10 m/s, respectively, for the Kitaev candidate material α-RuCl$_3$ with $J \simeq 100$ K [28,72–74] and $\kappa/J \simeq 0.05$ [75]. While the field strength is larger than that given by recent STM technique generating nanoscale magnetic fields at present [76], our study will provide a possible route to spatiotemporal manipulation of a vison and stimulate the development of experimental research. Here, we propose several routes to reduce the required magnetic field. Based on the present study, we find that A_{cr} decreases with increasing κ as shown in Fig. 3(e), suggesting that the increase of the uniform effective field results in the reduction of the required field strength. We have also confirmed that extending the region of an applied local field also enables manipulating a vison in lower local fields. This phenomenon originates from the presence of multiple sites at which the local fields contribute to the hopping of a vison [55,64]. Furthermore, selecting candidate materials with smaller energy scales of the Kitaev interaction [29,77] is also effective to reduce the the required field strength.

In summary, we have demonstrated that a vison accompanied by a Majorana zero mode can be manipulated spatiotemporally by a locally applied magnetic field sweeping in the Kitaev model under a uniform effective field. Increasing the intensities of the local and uniform fields enhances controllability due to interactions between visons and itinerant Majorana fermions. Notably, the vison gap plays a crucial role in the stable manipulation of a vison. Our finding sheds light on the impact of many-body effects of fractional quasiparticles on the vison manipulation and paves the way for achieving topological quantum computation in Kitaev spin liquids.

---

[1] E. Majorana, Teoria simmetrica dell'elettrone e del positrone, Nuovo Cimento **14**, 171 (1937).

[2] A. Y. Kitaev, Fault-tolerant quantum computation by anyons, Ann. Phys. (NY) **303**, 2 (2003).

[3] M. Freedman, A. Kitaev, M. Larsen, and Z. Wang, Topological quantum computation, Bull. Amer. Math. Soc. **40**, 31 (2003).

[4] C. Nayak, S. H. Simon, A. Stern, M. Freedman, and S. Das Sarma, Non-Abelian anyons and topological quantum computation, Rev. Mod. Phys. **80**, 1083 (2008).

[5] A. Ahlbrecht, L. S. Georgiev, and R. F. Werner, Implementation of Clifford gates in the Ising-Anyon topological quantum computer, Phys. Rev. A **79**, 032311 (2009).

[6] S. D. Sarma, C. Nayak, and S. Tewari, Proposal to stabilize and detect half-quantum vortices in strontium ruthenate thin films: Non-Abelian braiding statistics of vortices in a $p_x + ip_y$ superconductor, Phys. Rev. B **73**, 220502(R) (2006).

[7] M. Sato, Topological properties of spin-triplet superconductors and fermi surface topology in the normal state, Phys. Rev. B **79**, 214526 (2009).

[8] L. Fu and C. L. Kane, Superconducting proximity effect and Majorana fermions at the surface of a topological insulator, Phys. Rev. Lett. **100**, 096407 (2008).

[9] M. Sato and S. Fujimoto, Majorana fermions and topology in superconductors, J. Phys. Soc. Jpn. **85**, 072001 (2016).

[10] M. Sato and Y. Ando, Topological superconductors: A review, Rep. Prog. Phys. **80**, 076501 (2017).

[11] G. Moore and N. Read, Non-Abelions in the fractional quantum Hall effect, Nucl. Phys. B **360**, 362 (1991).

[12] H. L. Stormer, D. C. Tsui, and A. C. Gossard, The fractional quantum Hall effect, Rev. Mod. Phys. **71**, S298 (1999).

[13] N. Read and D. Green, Paired states of fermions in two dimensions with breaking of parity and time-reversal symmetries and the fractional quantum Hall effect, Phys. Rev. B **61**, 10267 (2000).

[14] M. Banerjee, M. Heiblum, V. Umansky, D. E. Feldman, Y. Oreg, and A. Stern, Observation of half-integer thermal Hall conductance, Nature (London) **559**, 205 (2018).

[15] A. Kitaev, Anyons in an exactly solved model and beyond, Ann. Phys. (NY) **321**, 2 (2006).

[16] Z. Nussinov and J. van den Brink, Compass models: Theory and physical motivations, Rev. Mod. Phys. **87**, 1 (2015).

[17] M. Hermanns, I. Kimchi, and J. Knolle, Physics of the Kitaev model: Fractionalization, dynamic correlations, and material connections, Annu. Rev. Condens. Matter Phys. **9**, 17 (2018).

[18] J. Knolle and R. Moessner, A field guide to spin liquids, Annu. Rev. Condens. Matter Phys. **10**, 451 (2019).

[19] H. Takagi, T. Takayama, G. Jackeli, G. Khaliullin, and S. E. Nagler, Concept and realization of Kitaev quantum spin liquids, Nat. Rev. Phys. **1**, 264 (2019).

[20] L. Janssen and M. Vojta, Heisenberg-Kitaev physics in magnetic fields, J. Phys.: Condens. Matter **31**, 423002 (2019).

[21] Y. Motome and J. Nasu, Hunting Majorana fermions in Kitaev magnets, J. Phys. Soc. Jpn. **89**, 012002 (2020).

[22] C. Hickey and S. Trebst, Kitaev materials, Phys. Rep. **950**, 1 (2022).

[23] G. Jackeli and G. Khaliullin, Mott insulators in the strong spin-orbit coupling limit: From Heisenberg to a quantum compass and Kitaev models, Phys. Rev. Lett. **102**, 017205 (2009).

[24] J. Chaloupka, G. Jackeli, and G. Khaliullin, Kitaev-Heisenberg model on a honeycomb lattice: Possible exotic phases in iridium oxides A_2IrO_3, Phys. Rev. Lett. **105**, 027204 (2010).

[25] J. Chaloupka, G. Jackeli, and G. Khaliullin, Zigzag magnetic order in the iridium oxide Na_2IrO_3, Phys. Rev. Lett. **110**, 097204 (2013).

[26] Y. Yamaji, Y. Nomura, M. Kurita, R. Arita, and M. Imada, First-principles study of the honeycomb-lattice iridates Na_2IrO_3 in the presence of strong spin-orbit interaction and electron correlations, Phys. Rev. Lett. **113**, 107201 (2014).

[27] J. G. Rau, E. K.-H. Lee, and H.-Y. Kee, Generic spin model for the honeycomb iridates beyond the Kitaev limit, Phys. Rev. Lett. **112**, 077204 (2014).

[28] S. M. Winter, Y. Li, H. O. Jeschke, and R. Valentí, Challenges in design of Kitaev materials: Magnetic interactions from competing energy scales, Phys. Rev. B **93**, 214431 (2016).

[29] M. G. Yamada, H. Fujita, and M. Oshikawa, Designing Kitaev spin liquids in metal-organic frameworks, Phys. Rev. Lett. **119**, 057202 (2017).

[30] L.-M. Duan, E. Demler, and M. D. Lukin, Controlling spin exchange interactions of ultracold atoms in optical lattices, Phys. Rev. Lett. **91**, 090402 (2003).

[31] S. R. Manmana, E. M. Stoudenmire, K. R. A. Hazzard, A. M. Rey, and A. V. Gorshkov, Topological phases in ultracold polar-molecule quantum magnets, Phys. Rev. B **87**, 081106(R) (2013).

[32] A. V. Gorshkov, K. R. Hazzard, and A. M. Rey, Kitaev honeycomb and other exotic spin models with polar molecules, Mol. Phys. **111**, 1908 (2013).

[33] K. Fukui, Y. Kato, J. Nasu, and Y. Motome, Feasibility of Kitaev quantum spin liquids in ultracold polar molecules, Phys. Rev. B **106**, 014419 (2022).

[34] Y. Kasahara, T. Ohnishi, Y. Mizukami, O. Tanaka, S. Ma, K. Sugii, N. Kurita, H. Tanaka, J. Nasu, Y. Motome, T. Shibauchi, and Y. Matsuda, Majorana quantization and half-integer thermal quantum Hall effect in a Kitaev spin liquid, Nature (London) **559**, 227 (2018).

[35] T. Yokoi, S. Ma, Y. Kasahara, S. Kasahara, T. Shibauchi, N. Kurita, H. Tanaka, J. Nasu, Y. Motome, C. Hickey *et al.*, Half-integer quantized anomalous thermal Hall effect in the Kitaev material candidate α-$RuCl_3$, Science **373**, 568 (2021).

[36] M. Yamashita, J. Gouchi, Y. Uwatoko, N. Kurita, and H. Tanaka, Sample dependence of half-integer quantized thermal hall effect in the Kitaev spin-liquid candidate α-$RuCl_3$, Phys. Rev. B **102**, 220404(R) (2020).

[37] J. Bruin, R. Claus, Y. Matsumoto, N. Kurita, H. Tanaka, and H. Takagi, Robustness of the thermal Hall effect close to half-quantization in α-$RuCl_3$, Nat. Phys. **18**, 401 (2022).

[38] R. Hentrich, M. Roslova, A. Isaeva, T. Doert, W. Brenig, B. Büchner, and C. Hess, Large thermal Hall effect in α-$RuCl_3$: Evidence for heat transport by Kitaev-Heisenberg paramagnons, Phys. Rev. B **99**, 085136 (2019).

[39] P. Czajka, T. Gao, M. Hirschberger, P. Lampen-Kelley, A. Banerjee, N. Quirk, D. Mandrus, S. Nagler, and N. P. Ong, Planar thermal Hall effect of topological bosons in the Kitaev magnet α-$RuCl_3$, Nat. Mater. **22**, 36 (2023).

[40] E. Lefrançois, G. Grissonnanche, J. Baglo, P. Lampen-Kelley, J.-Q. Yan, C. Balz, D. Mandrus, S. E. Nagler, S. Kim, Y.-J. Kim, N. Doiron-Leyraud, and L. Taillefer, Evidence of a phonon Hall effect in the Kitaev spin liquid candidate α-$RuCl_3$, Phys. Rev. X **12**, 021025 (2022).

[41] J. Feldmeier, W. Natori, M. Knap, and J. Knolle, Local probes for charge-neutral edge states in two-dimensional quantum magnets, Phys. Rev. B **102**, 134423 (2020).

[42] E. J. König, M. T. Randeria, and B. Jäck, Tunneling spectroscopy of quantum spin liquids, Phys. Rev. Lett. **125**, 267206 (2020).

[43] R. G. Pereira and R. Egger, Electrical access to Ising anyons in Kitaev spin liquids, Phys. Rev. Lett. **125**, 227202 (2020).

[44] G. Chen and J. L. Lado, Impurity-induced resonant spinon zero modes in Dirac quantum spin liquids, Phys. Rev. Res. **2**, 033466 (2020).

[45] M. Carrega, I. J. Vera-Marun, and A. Principi, Tunneling spectroscopy as a probe of fractionalization in two-dimensional magnetic heterostructures, Phys. Rev. B **102**, 085412 (2020).

[46] M. Udagawa, S. Takayoshi, and T. Oka, Scanning tunneling microscopy as a single Majorana detector of Kitaev's chiral spin liquid, Phys. Rev. Lett. **126**, 127201 (2021).

[47] S.-H. Jang, Y. Kato, and Y. Motome, Vortex creation and control in the Kitaev spin liquid by local bond modulations, Phys. Rev. B **104**, 085142 (2021).

[48] T. Bauer, L. R. D. Freitas, R. G. Pereira, and R. Egger, Scanning tunneling spectroscopy of Majorana zero modes in a Kitaev spin liquid, Phys. Rev. B **107**, 054432 (2023).

[49] K. Klocke, D. Aasen, R. S. K. Mong, E. A. Demler, and J. Alicea, Time-domain anyon interferometry in Kitaev honeycomb spin liquids and beyond, Phys. Rev. Lett. **126**, 177204 (2021).

[50] Z. Wei, V. F. Mitrović, and D. E. Feldman, Thermal interferometry of anyons in spin liquids, Phys. Rev. Lett. **127**, 167204 (2021).

[51] Y. Liu, K. Slagle, K. S. Burch, and J. Alicea, Dynamical anyon generation in kitaev honeycomb non-Abelian spin liquids, Phys. Rev. Lett. **129**, 037201 (2022).

[52] D. Takikawa and S. Fujimoto, Impact of off-diagonal exchange interactions on the Kitaev spin-liquid state of α-$RuCl_3$, Phys. Rev. B **99**, 224409 (2019).

[53] D. Takikawa and S. Fujimoto, Topological phase transition to abelian anyon phases due to off-diagonal exchange interaction in the Kitaev spin liquid state, Phys. Rev. B **102**, 174414 (2020).

[54] D. Takikawa, M. G. Yamada, and S. Fujimoto, Dissipationless spin current generation in a Kitaev chiral spin liquid, Phys. Rev. B **105**, 115137 (2022).

[55] C. Chen and I. S. Villadiego, Nature of visons in the perturbed ferromagnetic and antiferromagnetic Kitaev honeycomb models, Phys. Rev. B **107**, 045114 (2023).

[56] M. O. Takahashi, M. G. Yamada, M. Udagawa, T. Mizushima, and S. Fujimoto, Nonlocal spin correlation as a signature of Ising anyons trapped in vacancies of the Kitaev spin liquid, Phys. Rev. Lett. **131**, 236701 (2023).

[57] W.-H. Kao, N. B. Perkins, and G. B. Halász, Vacancy spectroscopy of non-Abelian Kitaev spin liquids, arXiv:2307.10376.

[58] H.-D. Chen and J. Hu, Exact mapping between classical and topological orders in two-dimensional spin systems, Phys. Rev. B **76**, 193101 (2007).

[59] X.-Y. Feng, G.-M. Zhang, and T. Xiang, Topological characterization of quantum phase transitions in a spin-1/2 model, Phys. Rev. Lett. **98**, 087204 (2007).

[60] H.-D. Chen and Z. Nussinov, Exact results of the Kitaev model on a hexagonal lattice: Spin states, string and brane correlators, and anyonic excitations, J. Phys. A **41**, 075001 (2008).

[61] J. Nasu, M. Udagawa, and Y. Motome, Vaporization of Kitaev spin liquids, Phys. Rev. Lett. **113**, 197205 (2014).

[62] J. Nasu, M. Udagawa, and Y. Motome, Thermal fractionalization of quantum spins in a Kitaev model: Temperature-linear specific heat and coherent transport of Majorana fermions, Phys. Rev. B **92**, 115122 (2015).

[63] T. Minakawa, Y. Murakami, A. Koga, and J. Nasu, Majorana-mediated spin transport in Kitaev quantum spin liquids, Phys. Rev. Lett. **125**, 047204 (2020).

[64] A. P. Joy and A. Rosch, Dynamics of visons and thermal Hall effect in perturbed Kitaev models, Phys. Rev. X **12**, 041004 (2022).

[65] See Supplemental Material at http://link.aps.org/supplemental/10.1103/PhysRevB.108.L241118 for the time-dependent Hartree-Fock theory, local-field dependence of vison transport, and time evolution in the low-energy effective model.

[66] A. F. Volkov and Sh. M. Kogan, Ocollisionless relaxation of the energy gap in superconductors, Sov. Phys. JETP **38**, 1018 (1974).

[67] N. Tsuji and H. Aoki, Theory of anderson pseudospin resonance with Higgs mode in superconductors, Phys. Rev. B **92**, 064508 (2015).

[68] Y. Murakami, D. Golež, T. Kaneko, A. Koga, A. J. Millis, and P. Werner, Collective modes in excitonic insulators: Effects of electron-phonon coupling and signatures in the optical response, Phys. Rev. B **101**, 195118 (2020).

[69] J. Nasu, Y. Murakami, and A. Koga, Scattering phenomena for spin transport in a Kitaev spin liquid, Phys. Rev. B **106**, 024411 (2022).

[70] We find that $D_1^{\max}$ decreases with increasing A for small κ, as shown in Fig. 3(d). Phenomenologically, this is considered to arise from Majorana fermions excited by strong magnetic fields because the behavior becomes less pronounced by an increase of κ that produces a widening of the Majorana gap.

[71] V. Lahtinen, Interacting non-Abelian anyons as Majorana fermions in the honeycomb lattice model, New J. Phys. **13**, 075009 (2011).

[72] A. Banerjee, C. A. Bridges, J. Q. Yan, A. A. Aczel, L. Li, M. B. Stone, G. E. Granroth, M. D. Lumsden, Y. Yiu, J. Knolle, S. Bhattacharjee, D. L. Kovrizhin, R. Moessner, D. A. Tennant, D. G. Mandrus, and S. E. Nagler, Proximate Kitaev quantum spin liquid behaviour in a honeycomb magnet, Nat. Mater. **15**, 733 (2016).

[73] S.-H. Do, S.-Y. Park, J. Yoshitake, J. Nasu, Y. Motome, Y. S. Kwon, D. Adroja, D. Voneshen, K. Kim, T.-H. Jang *et al.*, Majorana fermions in the Kitaev quantum spin system α-RuCl$_3$, Nat. Phys. **13**, 1079 (2017).

[74] D. Hirobe, M. Sato, Y. Shiomi, H. Tanaka, and E. Saitoh, Magnetic thermal conductivity far above the Néel temperature in the Kitaev-magnet candidate α-RuCl$_3$, Phys. Rev. B **95**, 241112(R) (2017).

[75] O. Tanaka, Y. Mizukami, R. Harasawa, K. Hashimoto, K. Hwang, N. Kurita, H. Tanaka, S. Fujimoto, Y. Matsuda, E. G. Moon, and T. Shibauchi, Thermodynamic evidence for a field-angle-dependent Majorana gap in a Kitaev spin liquid, Nat. Phys. **18**, 429 (2022).

[76] A. Singha, P. Willke, T. Bilgeri, X. Zhang, H. Brune, F. Donati, A. J. Heinrich, and T. Choi, Engineering atomic-scale magnetic fields by dysprosium single atom magnets, Nat. Commun. **12**, 4179 (2021).

[77] S.-H. Jang, R. Sano, Y. Kato, and Y. Motome, Computational design of f-electron Kitaev magnets: Honeycomb and hyper-honeycomb compounds A_2PrO$_3$ (A = alkali metals), Phys. Rev. Mater. **4**, 104420 (2020).